frontiers in Materials

ORIGINAL RESEARCH
published: 28 February 2022
doi: 10.3389/fmats.2022.823545

Novel Stimuli-Responsive Pectin-PVP-Functionalized Clay Based Smart Hydrogels for Drug Delivery and Controlled Release Application

Shabnam Rehmat[1,2], Nayab Batool Rizvi[1], Saba Urooge Khan[3], Abdul Ghaffar[4], Atif Islam[3]*, Rafi Ullah Khan[3], Azra Mehmood[5], Hira Butt[5] and Muhammad Rizwan[6]*

[1]School of Chemistry, University of the Punjab, Lahore, Pakistan, [2]HEJ Research Institute of Chemistry, International Center for Chemical and Biological Sciences, University of Karachi, Karachi, Pakistan, [3]Institute of Polymer and Textile Engineering, University of the Punjab, Lahore, Pakistan, [4]Department of Chemistry, University of Engineering and Technology, Lahore, Pakistan, [5]Center of Excellence in Molecular Biology, University of the Punjab, Punjab, Pakistan, [6]Department of Biomedical Engineering, Michigan Technological University, Houghton, MI, United States

OPEN ACCESS

Edited by:
Wenbo Wang,
Inner Mongolia University, China

Reviewed by:
Maria Emilia Villanueva,
Consejo Nacional de Investigaciones Científicas y Técnicas (CONICET), Argentina
Mohamed El-Aassar,
Jouf University, Saudi Arabia

***Correspondence:**
Shabnam Rehmat
shabnamrehmat123@gmail.com
Atif Islam
dratifislam@gmail.com

Specialty section:
This article was submitted to Polymeric and Composite Materials, a section of the journal Frontiers in Materials

Received: *27 November 2021*
Accepted: *05 January 2022*
Published: *28 February 2022*

Citation:
Rehmat S, Rizvi NB, Khan SU, Ghaffar A, Islam A, Khan RU, Mehmood A, Butt H and Rizwan M (2022) Novel Stimuli-Responsive Pectin-PVP-Functionalized Clay Based Smart Hydrogels for Drug Delivery and Controlled Release Application. Front. Mater. 9:823545. doi: 10.3389/fmats.2022.823545

Stimuli-responsive drug delivery systems are urgently required for injectable site-specific delivery and release of drugs in a controlled manner. For this purpose, we developed novel pH-sensitive, biodegradable, and antimicrobial hydrogels from bio-macromolecule pectin, polyvinylpyrrolidone (PVP), 3-aminopropyl (diethoxy)methyl silane (3-APDEMS), and sepiolite clay via blending and solution casting technique. The purified sepiolite (40 um) was functionalized with 3-APDEMS crosslinker (*ex-situ* modification) followed by hydrogels fabrication. FTIR and SEM confirmed crosslinked structural integrity and rod-like morphology of hydrogels respectively. The swelling properties of hydrogels could be controlled by varying the concentration of modified clay in pectin/PVP blends. Moreover, the decrease in pH increased the swelling of hydrogels indicating the pH-responsiveness of hydrogels. All hydrogels were degraded after 21 days in phosphate buffer saline pH 7.4 (human blood pH). *In-vitro* cytotoxicity against 3T3 mouse fibroblast cell line analysis confirmed cytocompatibility of all hydrogels. Ceftriaxone sodium (CTX-S) was selected as a model drug. The release profile of the hydrogel showed 91.82% release in PBS for 2 h in a consistent and controlled manner. The chemical structure of the drug remained intact during and after release confirmed through UV-Visible spectroscopy. Overall, these hydrogels could be used as potential scaffolds for future biomedical applications.

Keywords: hydrogel, pectin, 3-aminopropyl (diethoxy) methylsilane, polyvinylpyrrolidone, drug delivery, pH-responsive

1 INTRODUCTION

Conventional methods of drug delivery lead to the diffusion of drugs evenly throughout the body causing considerable damage to normal cells while reducing bioavailability. To overcome unfavorable actions, site-specific distribution of therapeutic medicine is essential. The smart hydrogel-based drug carriers can offer distinct advantages as targeted delivery (Raza et al., 2021), site-specificity, slow release of the drug, drug stability, optimized drug absorption, physiochemical compatibility with drug, non-

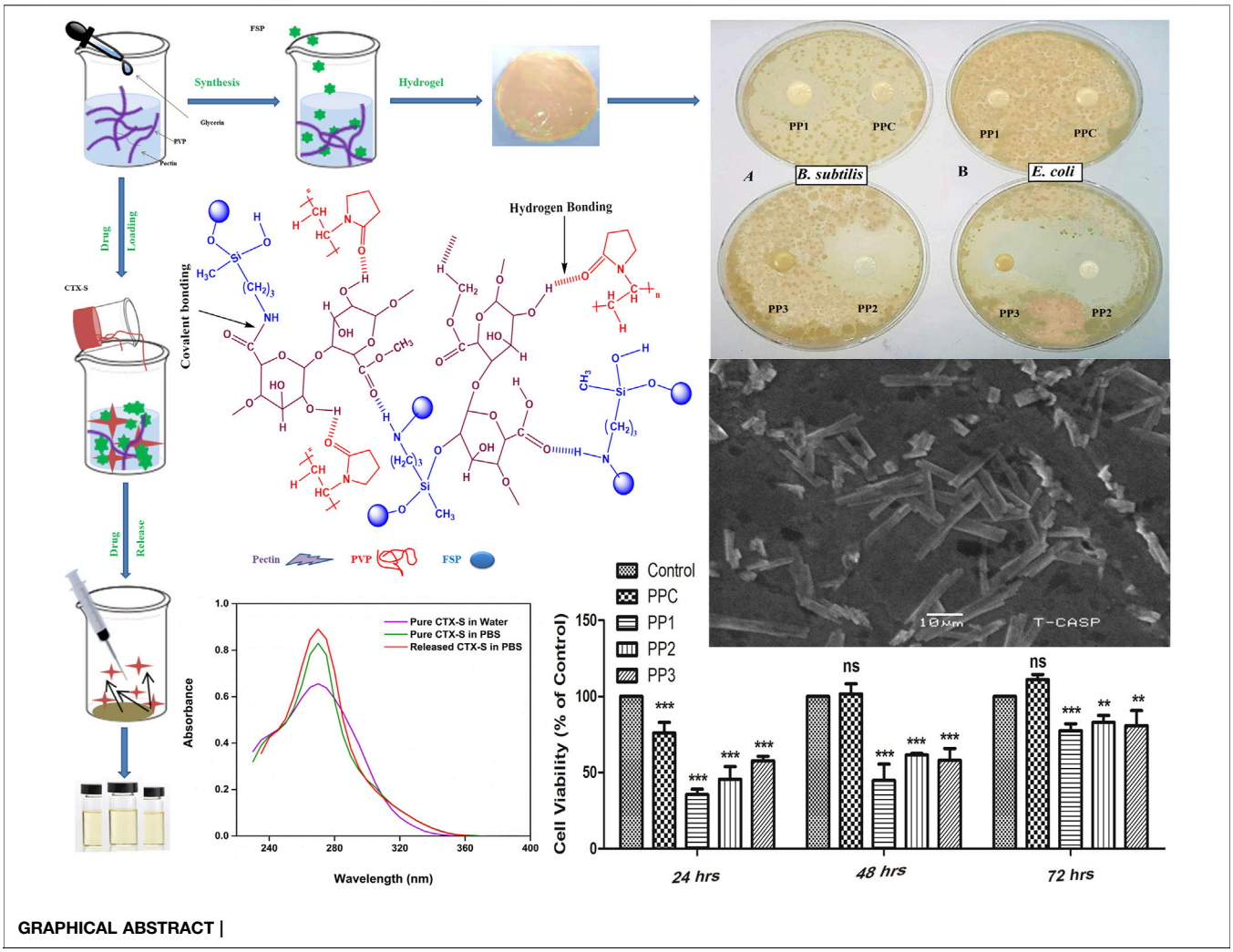

GRAPHICAL ABSTRACT |

toxicity, and biodegradability (Veronovski et al., 2014; Rasool et al., 2019; Peers et al., 2020; Ko et al., 2021; Liu et al., 2021). A variety of polymer-based stimuli-responsive (pH, temperature, light, enzymes, electricity, ultrasound, glucose) hydrogels have been synthesized (Yang et al., 2009; Peers et al., 2020; Liu et al., 2021; Song et al., 2021) due to their high swelling rate, soft tissue compatibility, and capability to prevent chemical and enzyme degradation (Islam and Yasin, 2012; Iglesias et al., 2020; Shirazi et al. 2021). Polymeric chains crosslink to develop microporous three-dimensional semi-interpenetrating networks (semi-IPNs) called hydrogel by penetrating at least one suitable linear or branched polymer (Liu et al., 2003; Mishra et al., 2008; Sivagangi Reddy et al., 2016; Rinoldi et al., 2021). Polysaccharides and their derivatives are among the ideal candidates for smart hydrogel formation due to stimuli-responsive behavior, reducing dose frequency, nontoxicity, stability, biocompatibility, biodegradability, easy availability, and cost-effectiveness (Roy et al., 2010; Sharma and Ahuja, 2011).

Pectin is an anionic, acidic, water-soluble, pH-sensitive, and fruit extracted polysaccharide (Mishra et al., 2008; Sriamornsak et al., 2008; Pierce et al., 2020). Its ability to naturally turn into gel, stabilize and thicken makes it a promising candidate for drug delivery application (Sharma and Ahuja, 2011; Veronovski et al., 2014). Pectin polysaccharide-based drug carriers direct the controlled release of therapeutic agents to achieve efficient treatment (Li et al., 2020; Li et al., 2021). However, pectin is a great choice for hydrogel formation however they show instant release of the drug, low thermal stability, and poor mechanical properties (Mishra et al., 2008; Li et al., 2020). Blending pectin with polymer like polyvinylpyrrolidone (PVP) offers the solution to these obstacles (Ghasemiyeh and Mohammadi-Samani, 2021). It is a hydrophilic synthetic polymer with tremendous solubility, low toxicity, biological compatibility (Eid et al., 2012; Singh and Singh, 2020), and excellent hydrogel film-forming properties. It has been reported to improve the mechanical characteristics of the hydrogel for various biomedical applications (Sizílio et al., 2018; Saeedi Garakani et al., 2020; Kumar et al., 2020).

Mishra et al. (2008) developed and examined the efficiency of pectin-based hydrogels prepared with different PVP ratios *via*

solution casting method for salicylic acid drug release (Mishra et al., 2008). Hussain et al. (2018) reported pH-dependent pectin-based nano-carriers functionalized with nano-graphene oxide for delivery of paclitaxel with better stability, higher drug loading efficiency, and non-toxicity (Hussien et al., 2018).

To improve hydrogel properties we used sepiolite (SP); a porous, lightweight reactive mineral clay (Nieto-Suárez et al., 2009) that has been reported as a reinforcing filler. It has been used as a pharmaceutical and medicinal ingredient for therapeutic purposes (Hun Kim et al., 2016; Darder et al., 2017; Dutta and Devi, 2021). It has also been used for tissue engineering, bio-medicines, and drug delivery applications (Ruiz-Hitzky et al., 2010; Gülmen, Güvel, and Kızılcan 2015; Tanc and Orakdogen 2019). Pectin and PVP have enormous potential for chemical/physical modifications using crosslinking agents like silane-based cross-linkers (Marandi et al., 2008; Yasin et al., 2008; Mirzaei B et al., 2013). In this study we choose 3-aminopropyl (diethoxy)methylsilane crosslinker (Khramov et al., 2003). Its bifunctional property makes it appropriate for crosslinking the polymers (Sanaeepur et al., 2019; Zu et al., 2019). In the current report, ceftriaxone sodium (CTX-S) has been used as a model drug. It is a third-generation cephalosporin (Bali et al., 2018) antibiotic used to treat various bacterial infections including tuberculosis, cholera, pneumonia, urinary tract, and pelvic inflammatory infections.

Various methods have been reported for hydrogel formation including freeze thawing, complex coacervation, radiation grating, and solution casting (Gulrez et al., 2011). Solution casting method is easy, cost effective, and requires shorter time of preparation. It is convenient to control reaction conditions in this technique (Rahman et al., 2018). Pectin-PVP based hydrogels have been used for delivery of various drugs other than ceftriaxone sodium (Mishra et al., 2008).

In this work, the functionalization of sepiolite clay with bifunctional 3-amino (diethoxy) methyl silane (3-APDEMS) was performed to produce novel functionalized sepiolite clay (FSP) using crosslinker and its use to produce novel pectin/PVP/functionalized clay based hydrogel blends for the delivery of ceftriaxone sodium. According to the best of our knowledge, the modification of sepiolite with 3-APDEMS, development of pectin/PVP/modified clay based hydrogels and their use particularly for the delivery and controlled release of ceftriaxone sodium (CTX-S) has not been reported yet. The physical blending and solution casting technique was adapted to develop novel pH-responsive hydrogels composed of pectin/PVP/3-APDEMS-sepiolite. The effects of variant concentrations of functionalized clay (FSP) on the characteristics of fabricated hydrogel were analyzed through FTIR and SEM. The swelling response of all the hydrogels was examined in water, ionic solutions (NaCl, $CaCl_2$), and buffers of varying pH. Biodegradation was observed in PBS for 21 days along with the antimicrobial activity. *In-vitro* toxicology for all hydrogels was assessed through XTT assay against 3T3 mouse fibroblast cell line. The chemical activity was performed to check the drug stability as well. The drug release pattern of CTX-S was investigated in phosphate buffer saline (PBS), simulated gastric fluid (SGF), and simulated intestinal fluid (SIF) via UV-vis spectroscopy.

2 EXPERIMENTAL WORK

2.1 Materials

Pectin (M. W = 1,61, 254, 94 g/mol) (low methoxy content), PVP (M. W = 40,000–70,000 g/mol), 3-aminopropyl (diethoxy) methylsilane (97%; MW = 191.34 g/mol) and sepiolite were obtained from Sigma Aldrich. Glycerin and ceftriaxone sodium were obtained locally. NaCl (sodium chloride), $CaCl_2$ (calcium chloride), Na_2HPO_4 (Disodium hydrogen phosphate), KH_2PO4 (potassium dihydrogen phosphate), and KCl (potassium chloride) were also purchased from Sigma-Aldrich. NaOH (sodium hydroxide) and $C_3H_2NaO_2$ (sodium acetate) were obtained from Riedel-de Haen. Ethanol and hydrochloric acid were purchased from BDH laboratory supplies and J.T. Baker, respectively. XTT (Cytotoxicity Detection assay kit II) was purchased from Roche, Germany. *B. subtilis* MH-4 (G+) strain, *E. coli* BL-21 (G-) strain, and LB agar were obtained from and Institute of Biochemistry and Biotechnology, University of the Punjab Lahore.

2.2 Modification of Sepiolite With 3-APDEMS

The *ex-situ* modification of clay was done according to the previously reported method (Shafiq et al., 2012). Sepiolite clay was purified by the mechanical stirring of the clay suspension (10 g/700 ml) for 24 h around 760 rpm. The resulting suspension was filtered and desiccated overnight at 105°C. The purified clay was grounded and sieved through 40 μm sieves. 5 g of purified raw sepiolite clay (RSP) was dispersed in 250 ml of isopropanol followed by mechanical stirring in the glass reactor. 500 μL of 3-APDEMS was solvated in 20 ml ethanol and added to RSP/isopropanol mixture. The suspension was stirred mechanically in a glass reactor for 2 h at 60°C. The functionalized clay was filtered followed by washing with ethanol. The *ex-situ* functionalized sepiolite clay (FSP) was dried up in a vacuum oven. The proposed reaction of sepiolite with 3-APDEMS is presented in **scheme 1**.

2.3 Fabrication of Hydrogels

Pectin (0.6 g) was solvated in double-distilled water (60 ml) at 60°C by magnetic stirring. PVP (0.4 g) was solvated in double-distilled water (20 ml) by magnetic stirring using a hot plate at 95°C. PVP solution was blended with the pectin solution with constant stirring for 2 h at 60°C. 200 μL of glycerin was added to the pectin-PVP blend upon stirring in order to prevent brittleness in the hydrogel. For crosslinking, varying amounts of FSP (3-APDEMS-sepiolite clay) ranging from 0.05–0.15 wt% were dispersed in 10 ml water and sonicated for 1 hour at an ambient temperature. Sonicated clay was poured into a pre-blended mixture drop wise and stirred magnetically for 2 h at 60°C. The fabricated hydrogels were cast in plates and desiccated using a desiccating oven (LVO-2040, Lab Tech, Korea) at 60°C under vacuum. Depending upon the concentration of modified functionalized clay (FSP), the hydrogels were referred to as control blend PPC (0 wt%), PP1 (0.05 wt%), PP2 (0.10 wt%), and PP3 (0.15 wt%). The treated hydrogels with sepiolite were: PP1, PP2, PP3 while the untreated was PPC which was controlled

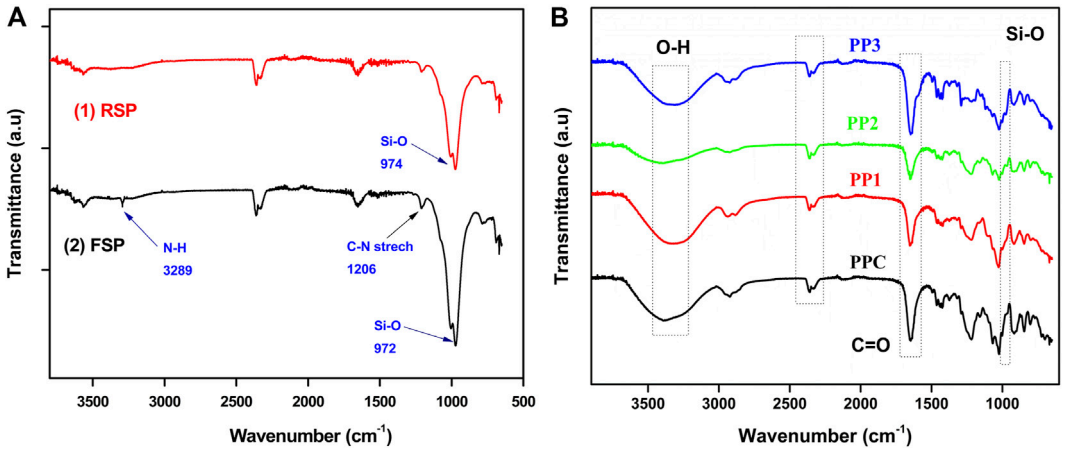

FIGURE 1 | (A) FTIR spectral analysis of modification of sepiolite clay with 3-APDEMS **(B)** FTIR spectral analysis of PPC, PP1, PP2, and PP3 semi-IPNs.

sample. The overall fabrication of hydrogels is shown in **scheme 2**.

2.4 Swelling Studies

To determine the swelling properties of prepared semi-IPNs, pre-weighed dried hydrogel samples were submerged in distilled water, NaCl and $CaCl_2$ salt solutions (0.1, 0.3, 0.5, 0.7, 0.9, and 1 M) and buffer solutions (pH 2, 4, 7, 7.4, and 8). The pH of all NaCl and $CaCl_2$ salt solutions was kept neutral. At a pre-set time interval, the swollen hydrogel was removed; the surplus solution was blotted gently and hydrogel was weighed using a sensitive weighing balance. This procedure was repeated in triplicates for all hydrogel samples in each solution.

The swelling rate was calculated using **Equation (1)**.

$$\text{Swelling } \% = (W_s - W_d/W_d)\times 100 \quad (1)$$

Where W_s = weight of swollen sample at time t and W_d = weight of sample in the dried state.

Buffer solutions of pH 2, 4, 7, 7.4, and eight were prepared to investigate the pH-dependent swelling response of hydrogels. To prepare buffer solutions of pH 2, 25 ml of 0.2 M KCl was mixed with 6.5 ml of 0.2 M HCl. For pH 4 solution, 50 ml of 0.1 M kH phthalate was mixed with 3 ml of 0.1 M NaOH. For pH 7 solution, 50 ml of 0.1 M KH_2PO_4 was mixed with 29.1 ml of 0.1 M NaOH. For pH 7.4 solution, 50 ml of 0.1 M KH_2PO_4 was mixed with 39.1 ml of 0.1 M NaOH. For pH eight solution, 50 ml of 0.1 M KH_2PO_4 was mixed with 46.1 ml of 0.1 M NaOH. All solutions were diluted up to 100 ml using distilled water.

2.5 FTIR Analysis

Spectroscopic structural elucidation of hydrogels, raw sepiolite (RSP), and functionalized sepiolite (FSP) was obtained on Shimadzu I. R–prestige-21, Kyoto, Kyoto prefecture, Japan with ATR mode. All films were vacuum dried before analysis and the scanning range was set as 4,000–650 cm^{-1}. Regular scans and resolution were maintained as 150 and 2.0 cm^{-1}, respectively.

2.6 Morphological Studies

The morphology of pectin/PVP (PPC) and pectin PVP/modified clay-based hydrogels (PP1, PP2, and PP3) was analyzed using model JEOL/EO JSM-6480 SEM Akishima, Tokyo, Japan. The images were recorded at different magnifications.

2.7 In-vitro Degradation

The biodegradation of all hydrogel samples was investigated in PBS (pH 7.4). Pre-weighed samples were placed for 21 days in PBS. All samples were weighed on days one, three, five, seven, fourteen, and twenty-one, respectively. The experiment was performed in triplicates. The percentage of degradation was measured using **Equation (2)**.

$$\text{Degradation}\,(\%) = (W_i - W_f/W_i)\times 100 \quad (2)$$

Where W_i = initial weight and W_f = final weight.

2.8 Antimicrobial Analysis

Agar disc diffusion assay (Mathew, 2018) was performed to investigate the anti-bacterial potential of all hydrogels against *B. subtilis* MH-4 and *E. coli* BL-21. Approximately, 5 mm disc-shaped sample of each hydrogel was cut. Bacterial culture was grown over 24 h in the form of suspension. 100 µL of bacterial suspension was transferred to sterilized LB agar plates. Aseptically, the hydrogel samples were transported to agar plates. Air was considered as negative control. The culture plates were incubated in the static incubator at 37°C for the next 24 h. The inhibition zones (clear zone) acted as an indicator for restricted bacterial growth around samples. The diameter of inhibition zones was recorded and measured.

2.9 Cytotoxicity Studies

The cytocompatibility of all hydrogels was investigated using Cytotoxicity Detection Kit II (XTT); Roche, Germany (XTT; sodium 3-[1- (phenylaminocarbonyl)- 3,4- tetrazolium]-bis (4-methoxy6-nitro) benzene sulfonic acid hydrate) (Jacob et al.,

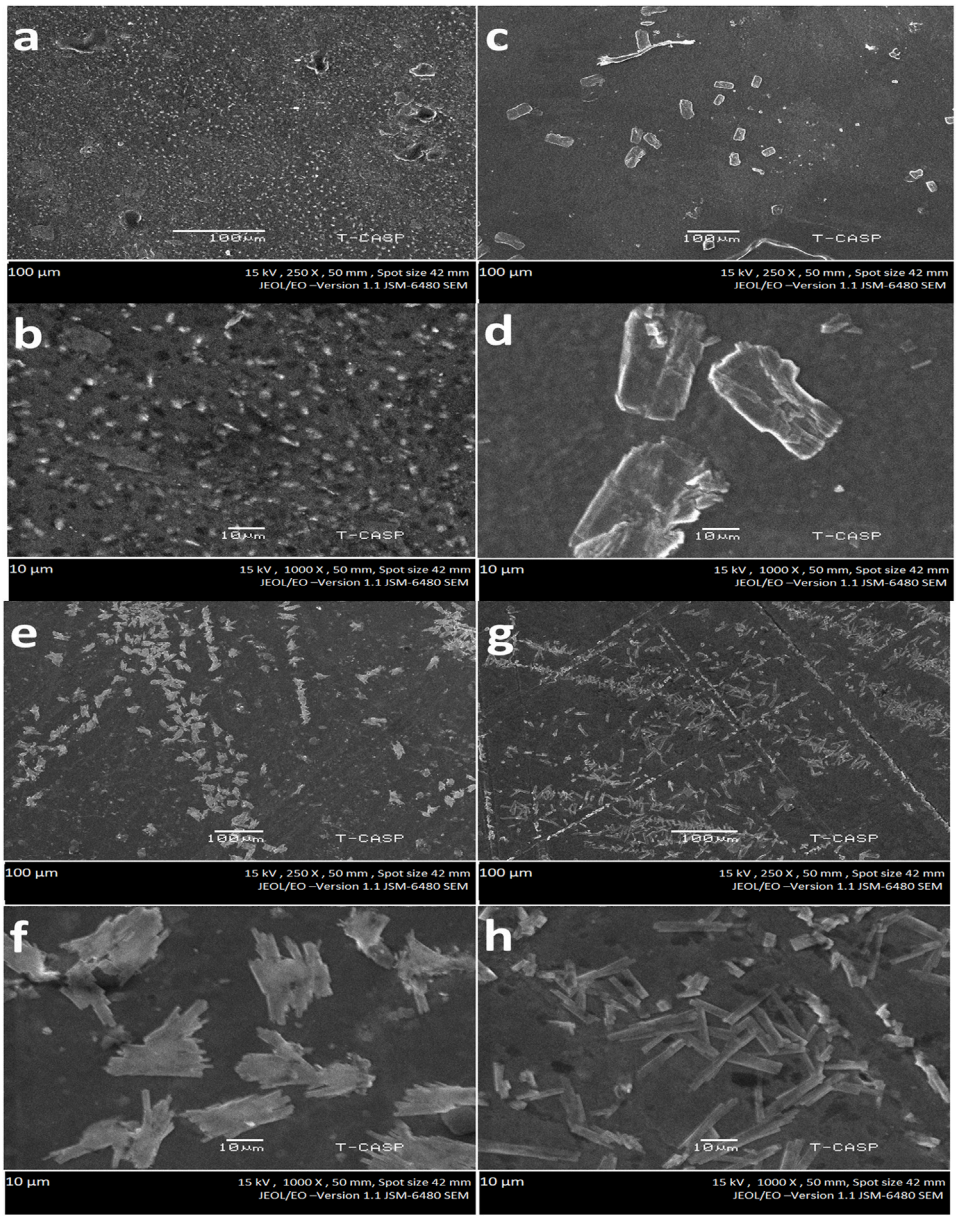

FIGURE 2 | Morphology of hydrogels at different magnifications **(A,B)**. PPC (Functionalized Sepiolite clay = 0 wt%) **(C,D)**. PP1(Functionalized Sepiolite clay = 0.05 wt%) **(E,F)** PP2 (Functionalized Sepiolite clay = 0.1 wt%) **(G,H)** PP3 (Functionalized Sepiolite clay = 0.15 wt%).

2020). The hydrogels were cut into the size of ~0.30 cm^2 and sterilized. After soaking the gel in a culture medium for half an hour, the cells at the density of 8,000 cells per well were seeded on the hydrogels. The cultured cells without hydrogel were used as control. XTT and PMS (electron coupling reagent) were mixed in a 50:1 ratio to form the labeling mixture. The cultured cells were incubated with 50 ul of labeling mixture and 100 ul of DMEM (containing 5% FBS) in 96-well plates for 24, 48, and 72 h under standardized conditions. Absorbance readout was determined at 450 and 630 nm (reference wavelength) using a microplate reader (Spectramax PLUS, United States) (Aguiar et al., 2017). The cell viability over time (24, 48, and 72 h) was measured in terms of percentage. The test was performed in triplicate.

2.10 Ceftriaxone Sodium (CTX-S Antibiotic Drug) Loading and Release Analysis

To investigate the release of drug from hydrogels the PBS, SGF, and SIF buffers were prepared. PBS (phosphate buffer saline pH 7.4) was synthesized by solvating NaCl (8 g), KCl (0.2 g), Na_2HPO_4 (1.44 g), and KH_2PO_4 (0.24 g) in 700 ml of distilled water and the volume was raised to 1 L. The pH was adjusted to

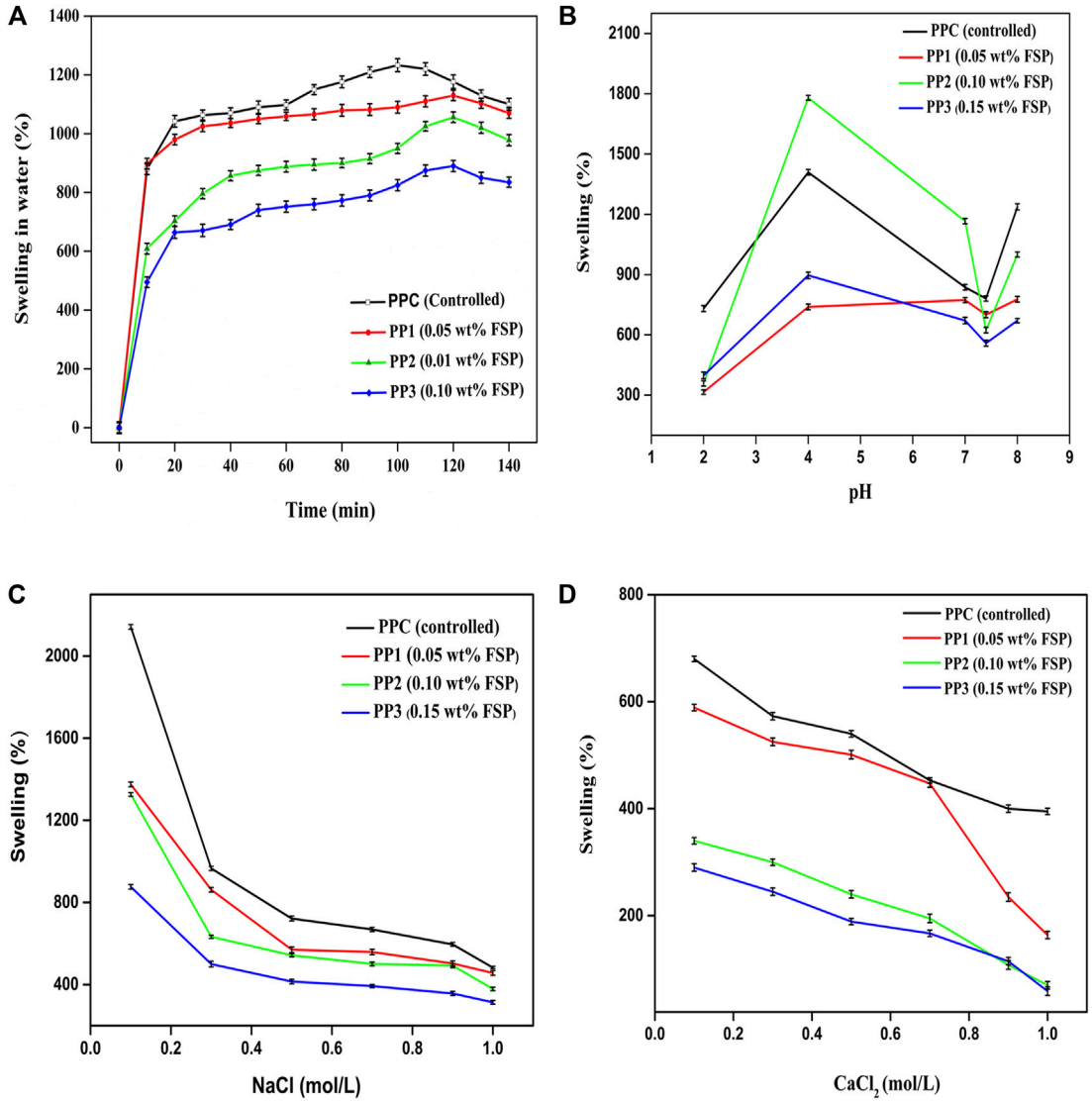

FIGURE 3 | (A) Time-dependent swelling behavior of PP hydrogel in water **(B)** pH-sensitive swelling response of PP hydrogels **(C)** swelling response of PP hydrogels against NaCl **(D)** swelling response of PP hydrogels against $CaCl_2$.

7.4. NaCl (1 g) and HCl (3.5 ml) were solvated in 100 ml of distilled water to prepare SGF (simulated gastric fluid pH 1.2). To adjust the pH to 1.2, the total volume was raised to 500 ml. To prepare SIF (simulated intestinal fluid pH 6.8), 0.1 M NaOH and 0.2 M KH_2PO_4 were mixed by 118 ml: 250 ml ratio. The pH of SIF was adjusted to 6.8.

CTX-S (50 mg) was liquefied in 5 ml H_2O and poured into the pectin-PVP mixture upon continuous stirring. The mixture was stirred for 1 h. The pectin-PVP/CTX-S mixture was crosslinked by the addition of 0.10g/10 ml sonicated suspension of 3-APDEMS-sepiolite (FSP). The antibiotic-containing solutions were cast and dried in an oven at 40°C. To examine the discharge pattern of CTX-S, the dried CTX-S-loaded hydrogels were immersed separately in 100 ml of solutions of PBS (pH 7.4), SGF (pH 1.2), and SIF (pH 6.8) at 37°C. At an equal interval of 10 min, 5 ml of release medium was collected in the glass vial and replaced with 5 ml of stock solution. Similar process was repeated over 4 h. The release of CTX-S was investigated at 241 nm (Ayushi and Mansi, 2018) using a V-730 UV-visible spectrophotometer (JASCO).

2.11 Chemical Activity

To investigate the effect of hydrogel on the chemical integrity of CTX-S before loading into the hydrogel and after release from hydrogel, the chemical activity of CTX-S was performed according to the previously described method (Bashir et al., 2018). The UV spectra of pure CTX-S in water, pure CTX-S in PBS, and CTX-S released in PBS, were obtained using a UV-Vis spectrophotometer (Model T90, Pg Instrumental) at the wavelength range 200–400 nm.

3 RESULTS AND DISCUSSION

Pectin has been used in drug delivery applications due to its antimicrobial potential, biocompatibility, nontoxicity, biodegradability, and swelling properties. Pectin produces physically crosslinked gel by hydrogen bonding, ionic association, or hydrophobic interactions (Ahrabi et al., 2000; Andrews et al., 2009). Sepiolite was functionalized with 3-APDEMS before addition to the pectin-PVP blends. The diverse effects of variant concentrations of 3-APDEMS-sepiolite (FSP) on the properties of fabricated semi-IPNs were investigated.

3.1 FTIR Analysis of Functionalized Sepiolite Clay and Fabricated Hydrogels

Previously reported method has been followed to modify sepiolite clay with 3-APDEMS (Shafiq et al., 2012). 3-APDEMS was used as the characteristic bifunctional crosslinker; its silanol groups reacted with -OH of sepiolite during modification and -NH_2 (amino) with polymer matrix during hydrogel fabrication via condensation. The proposed reaction of sepiolite with 3-APDEMS is presented in **scheme 1**. The addition of ethanol to 3-APDEMS activated the molecule by generating silanol sites (Si-OH) which reacted with sepiolite via condensation process to produce 3-APEMS functionalized sepiolite clay (FSP).

To investigate the modification of sepiolite the FTIR spectra of raw sepiolite (RSP) and functionalized sepiolite (FSP) were obtained. **Figure 1A** 1) represents the spectra of RSP and **Figure 1A** 2) shows spectra of FSP. In FSP, a characteristic peak appeared at 3,289 cm^{-1} which could be ascribed to the -NH stretch of 3-APDEMS confirming the modification of RSP (Xu et al., 1997). Another characteristic peak in FSP spectra at 1,210–1,150 cm^{-1} appeared which could be ascribed to the C-N stretch (Nandiyanto et al., 2019). The Si-O bond stretch can be seen at 974 cm^{-1} in RSP which was shifted to lower wavenumber 972 cm^{-1} in FSP (Shafiq et al., 2012). The increased intensity of the Si-O peak in FSP can also be observed. This increased intensity of the Si-O peak could be ascribed to the formation of new Si-O bonds during modification.

The varied concentration of FSP was added to polymer blends to fabricate hydrogels. **Scheme 3** presented the proposed crosslinking of FSP with pectin/PVP polymer matrix. FSP developed hydrogen bonding with pectin and PVP majorly through–OH and–NH_2 groups. The COOH of pectin could form covalent linkage with–NH_2 of FSP through condensation reaction.

To investigate the incorporation of polymers into the hydrogel polymer matrix, FTIR spectra of all hydrogels were recorded. Spectral analysis of all functional groups of hydrogels is presented in **Figure 1B**. The spectral analysis showed a band at 3,366–3,300 cm^{-1} indicated vibrations of polymer boneded -OH groups (Mishra et al., 2008; Naeem et al., 2017). Peaks at 1,420–1,460 cm^{-1} indicated the C-H bending vibrations. The peeks at 1,023–1,042 cm^{-1} showed the starching vibration of C-N of PVP within the hydrogel networks (Mishra et al., 2008; Kumar et al., 2010).

The distinctive doublet that appeared around 2,360–2,330 cm^{-1} might be due to adsorbed CO_2. However,

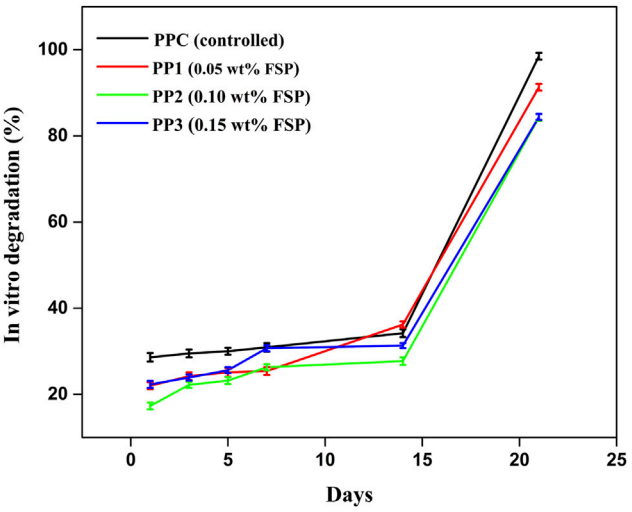

FIGURE 4 | *In-vitro* degradation analysis of PP hydrogels in PBS (pH 7).

Basha (2010) and Bryaskova et al. (2011) separately reported this distinctive doublet as characteristic peaks of pure PVP IR spectrum (Basha, 2010; Bryaskova et al., 2011) which indicated the incorporation of PVP in all hydrogels. The peaks around 2,970 cm^{-1} could be ascribed to the -CH_2 vibrations of PVP chain (Song et al., 2014) while the peaks at 1,625–1,660 cm^{-1} indicated the presence of C=O stretching vibrations in all hydrogels (Fares et al., 2010; Sohail et al., 2014). The Si-O stretching vibrations can be observed in PP1, PP2, and PP3 around 970 cm^{-1} (Shafiq et al., 2012) which shows the incorporation of modified sepiolite clay.

3.2 Morphological Analysis of Hydrogels via SEM

The morphological properties of fabricated hydrogels are highly dependent on the polymers and incorporated clay (Liu et al., 2020). Raw sepiolite clay (SP) exhibits rod/fiber-like morphology as evident from reported data (Abrougui et al., 2019). Evident from the work of Palem et al. (2021), a small concentration of raw sepiolite (fibrous clay) affects the morphology of composites by enhancing the interfacial interactions between the polymers and–OH of sepiolite layers (Palem et al., 2021; Liu et al., 2020). In this study, the sepiolite was first functionalized with bifunctional 3-APDEMS moiety then incorporated into the polymer matrix. The modified sepiolite clay (FSP) has both–NH_2 (from 3-APDEMS) and–OH groups (from 3-APDEMS and sepiolite) which can enhance the crosslinking density by a greater degree as compared to raw sepiolite, hence causing the drastic change in shape and size of the hydrogel. To investigate the possible effect of the reinforcement of FSP on the morphology of hydrogels with respect to the varied concentrations of FSP, SEM analysis was conducted. **Figures 2A–H** shows SEM micrographs of pectin/PVP control hydrogel (PPC with 0 wt%) and pectin/PVP/modified clay-based hydrogels (PP1, PP2, and PP3). Pure

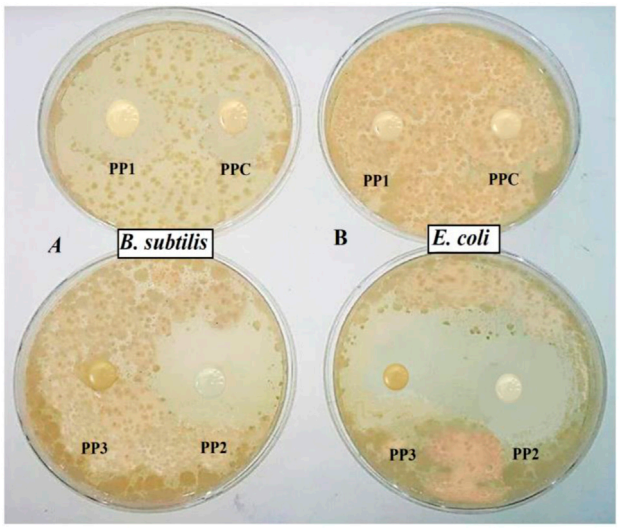

FIGURE 5 | Antimicrobial activity of fabricated hydrogels after 24 h against **(A)** *Bacillus subtilis* MH-4 (G+) **(B)** *Escherichia coli* BL-21 (G-).

pectin shows the elongated granular structure and pure PVP shows spherical granular shapes as it seems in literature (Kumar et al., 2010; Mishra et al., 2008). In our study the PPC (0 wt% FSP) is composed of pectin and PVP only thus spherical granular structures of PPC can be observed from the micrographs of PPC. While the SEM images of PP1 (0.05wt % FSP) and PP2 (0.1wt% FSP) showed capsule-type structures (10–50 μm) separated from one another. SEM micrographs of PP3 (0.15wt% FSP) showed a large population of refined, compact rod-like structures (10 μm). Moving from PPC to PP1 (**Figures 3A–D**), a clear change in the shape of particles from granular to capsule can be observed after the addition of 0.05 wt% FSP. The change in morphology from PP1 (0.05 wt% FSP) capsule structure to PP2 (0.10 wt% FSP) rod-like structure with a reduction in size of particle can be seen (**Figures 3C–F**). This change in morphology can be attributed to the increased concentration of FSP and the interfacial interactions between FSP and polymer networks. From PP2 (0.05 wt% FSP) to PP3 (0.15 wt% SP) (**Figures 3E–H**), the amount of clay, as well as the number of interfacial bonds, increased in PP3 caused the rod-like compact structure and increased shrinkage in particle size. This change in morphology of hydrogels with an increase in the concentration of FSP could be attributed to fibrous structure of FSP and enhanced covalent linkages and hydrogen bonding due to NH_2 and–OH of FSP throughout the hydrogel (Liu et al., 2020; Palem et al., 2021).

TABLE 1 | Antimicrobial potential of hydrogels in terms of inhibition zones.

Bacterial cultures	Diameter (d) of hollow zones formed (mm)			
—	PPC	PP1	PP2	PP3
E.coli BL-21	2	3	18	23
B.subtilis MH-4	5	9	16	0

3.3 Swelling Kinetics

To obtain a comprehensive understanding of swelling characteristics of newly developed hydrogels we tested swelling kinetics of all hydrogels in different media.

3.3.1 Swelling Response of Hydrogels in Water

The swelling response of PP hydrogel in water to time is demonstrated in **Figure 3A**. All the hydrogels presented different responses against water. The hydrogels exhibited an increase in swelling over time. The amount of crosslinker affected the swelling behavior of all films differently. In the controlled sample, maximum swelling (1,233%) was observed after 100 min while FSP incorporated samples showed maximum swelling as; PP1 (1,130%), PP2 (1,056%), PP3 (890%) after 120 min. All films started to dwell after reaching the respective equilibrium time.

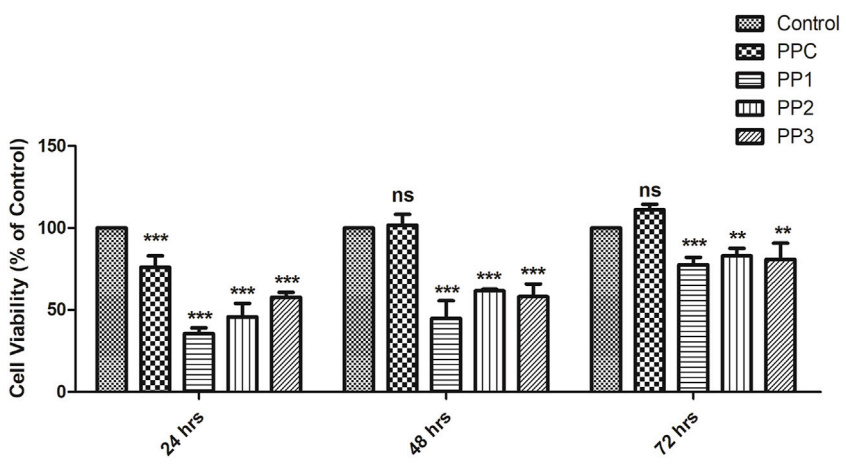

FIGURE 6 | Viability of 3T3 fibroblasts cells seeded in different groups of hydrogels determined by XTT assay. The control group (doted bar) represents 3T3 fibroblasts cells seeded without any hydrogel. Cells exhibit high viability indicating absence of cytotoxic effect of hydrogels. *p denotes statistical significance: *$p < 0.05$; **$p < 0.01$; ***$p < 0.001$.

Maximum swelling was exhibited by PPC and minimum swelling was shown by PP3. The decrease in swelling from PPC to PP3 could be attributed to the decreasing number of free pendent carboxyl and hydroxyl groups upon increasing the amount of crosslinker. The crosslinker might have caused the shrinkage of pores by increasing the crosslinking density and high chain interconnectivity leaving a fewer number of pores for diffusion of solvent into hydrogel matrix (Butt et al., 2019). With an increase in the amount of FSP, a clear decrease in the swelling trend was noticed.

3.3.2 Effect of pH on Swelling of Hydrogels

Different stimuli can cause unusual alterations in hydrogel swelling behavior, structure, and mechanical properties. The swelling extent of fabricated films is critically affected by the nature of base polymers, pH, and the type of buffer medium. For pH-dependent controlled release of the drug, the response of hydrogel swelling due to change in pH of medium particularly needs to be studied. The behavior of all hydrogels was checked in different pH solutions (pH 2, 4, 7, 7.4, and 8). **Figure 3B** depicts the pH-dependent swelling trend of all hydrogels. All hydrogels showed a minimum swelling rate at pH 2. With an increase in pH, an increase in swelling was observed, while at neutral pH the swelling was decreased. The swelling was again increased at basic pH. This was due to the charge imbalance caused by the pH of the buffer solution. At the pH value (pH 2) lower than the pKa value (3.55–4.10) of pectin, the pendent -COOH group of pectin did not lose its proton and remained uncharged resulting in low swelling. Furthermore, the hydrogen bonds were developed between the -OH of pectin and -C=O of PVP which instigated less swelling at said pH (Mishra et al., 2008). At pH (pH 4) equal to pKa of pectin, a few -COOH in the pectin backbone might be ionized by losing protons. This ionization caused intra-chain repulsive forces inducing hydrophilicity and increase in pore size causing the inward movement of solvent into the hydrogel through the process of diffusion resulting in an increase in swelling. (Butt et al., 2019). Maximum swelling of PPC (1,409%), PP1 (739%), PP2 (1780%), and PP3 (896%) was noted at the pH value equal to the pKa value of pectin. The increased extent of swelling in PP2 specifically at pH 4 might be due to the increased diffusion rate caused by the influence of salt concentration, type of salts present in the medium, and ionization of -COOH group at the pH value equal to the pKa value of pectin. Moving to neutral pH, the swelling of PP2 again decreased and minimized at pH 7.4 followed by a rise at basic pH. At basic pH 8) where the pH value of medium was much higher than the pKa value of pectin, the dissociation of hydrogen bonds and ionization of–COOH groups of pectin caused an increase in the swelling rate. The fabricated hydrogel films showed pH-dependent swelling. These films responded to the slight change in pH of the medium which can result in a change in hydrogel characteristics.

3.3.3 Effect of Ionic Concentration on Swelling of Hydrogels

The swelling response of hydrogels could be affected by the concentration of ions (Na^+ and Ca^{2+}) present in the blood. To investigate the possible effect of these ions on the swelling response of hydrogel was studied *in vitro* against different concentrations of sodium chloride and calcium chloride salt solutions under neutral pH conditions. The sodium chloride and calcium chloride are neutral salts. Upon dissolution in water both of these salts dissociated into cations (Na^+ and Ca^{2+}) and anions (Cl^-). **Figures 3C,D** depict the swelling response of all hydrogels in NaCl and $CaCl_2$ respectively. Both the NaCl and $CaCl_2$ electrolytes contain the same anion (Cl^-) but different cations; monovalent sodium ions and divalent calcium ions, respectively. **Figures 3C,D** indicated an observable decrease in the swelling rate of hydrogels with the rise in the electrolyte concentration. An increase in concentration increased the

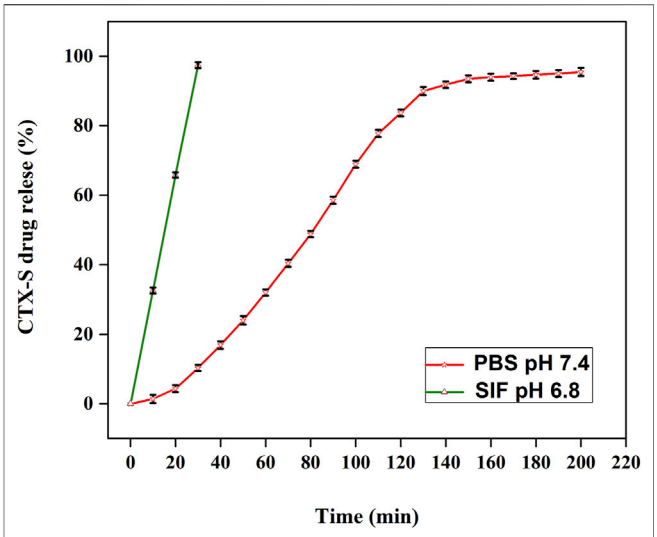

FIGURE 7 | The controlled *in vitro* release of CTX-S in PBS (pH 7.4) and SIF (pH 6.8).

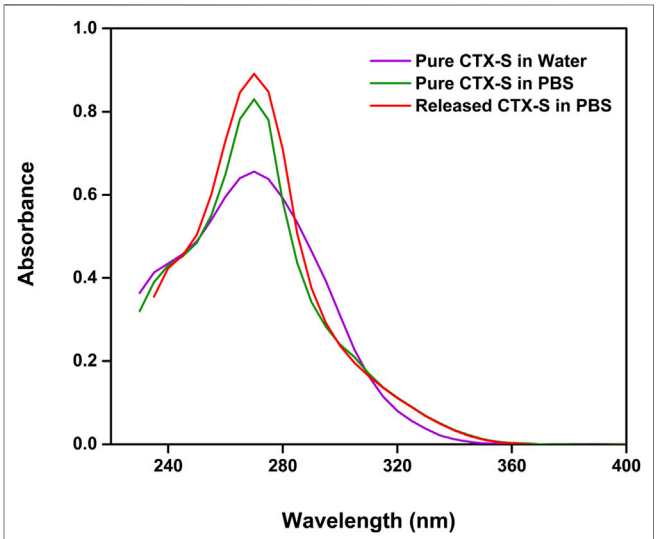

FIGURE 8 | The chemical activity of the pure CTX-S and after release from the hydrogel.

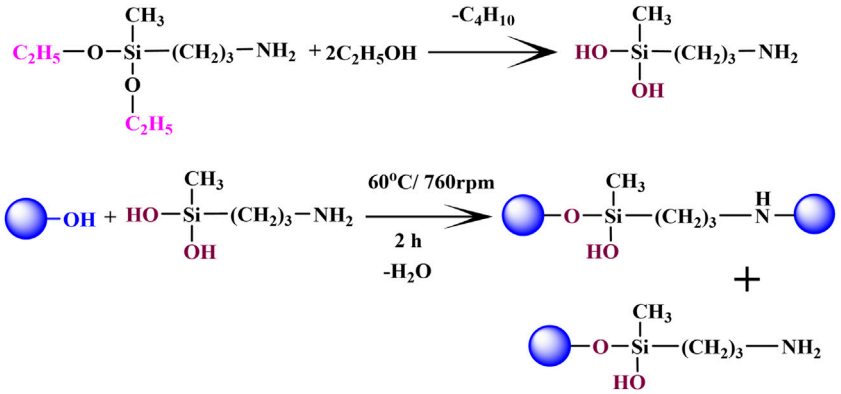

FIGURE 9 | Proposed reaction for modification of sepiolite with 3-APDEMS

osmotic pressure within the polymeric network. This osmotic pressure hindered the movement of solvent into the gel hence decreasing the swelling extent (Rasool et al., 2010; Rasool et al., 2019). The second factor affecting the swelling trend of films observed was the net charge of ions. The ionic charge on cations influenced the swelling of hydrogels in an inverse manner. As the ionic charge Ca^{+2} is higher than the charge on Na^{+1} thus all the hydrogels showed less swelling in calcium chloride solution in comparison with swelling in sodium chloride solutions. The inter-chain complexes caused the hydrogel to attain a more compact structure hindering the diffusion of the solvent into the hydrogel which decreased the swelling rate (Muller et al., 2003). The swelling of all hydrogels decreased with an increase in ionic concentration as well as ionic charge.

3.4 In-vitro Degradation

The fabricated hydrogels are mainly composed of pectin. The monomers of pectin are linked via glycosidic linkages which can be easily broken by various enzymes resulting in small polysaccharide chains. These chains are further broken down to incorporate into biological metabolic pathways. In this analysis, the *in-vitro* biodegradation of all semi-IPNs was examined in a PBS solution of pH 7.4 for 21 days. The outcomes are presented in **Figure 4** which depicted the extent of degradation of PP films (PPC = 98.5%, PP1 = 91.3%, PP2 = 84.3% and PP3 = 84.4%) with respect to time. The biodegradation of all PP hydrogels depended on the nature and concentration of pectin, PVP, and FSP crosslinker. **Figure 4** showed that with an increase in the amount of FSP, the extent of degradation was decreased which can be attributed to the increased inter and intra-molecular forces of attraction among the polymers and FSP (Giri et al., 2013). The PPC hydrogel without FSP exhibited a higher degree of degradation (lower % remaining weights) as compared to hydrogels crosslinked with FSP (PP1, PP2, and PP3). The FSP (functionalized sepiolite clay) hindered the diffusion of solvent through the polymer matrix in PP1, PP2, and PP3. Thus, an increase in crosslinking density upon an increase of FSP concentration impeded the degradation of semi-IPNs.

The *in vitro* degradation results of all hydrogels also depicted the stabilizing effect of modified clay on the pectin-PVP polymer matrix. **Figure 4** presents the PP3 (0.15 wt% FSP) showed the highest stability while PPC (0 wt% FSP) showed minimum stability in PBS over time. The stability of hydrogel increased with an increase in the concentration of modified clay which could be referred to the increased inter-chain crosslinking density of polymer matrix.

3.5 Antimicrobial Analysis

The antimicrobial activity was examined by measuring the inhibition zones generated around the hydrogel (Nešić et al., 2017). The antimicrobial activity of all hydrogels is presented in **Figure 5** while in **Table 1**, the inhibition zone diameters (d in mm) are described. The antimicrobial activity of all hydrogels was investigated against *B. subtilis* MH-4 (G+) and *E. coli* BL-21 (G-) via the disc diffusion method and air was considered as the negative control. The PPC (0 wt% FSP) and PP1 (0.05 wt% FSP) showed less activity (5ays and 9days, respectively) against *B. subtilis* and negligible activity (2ays and 3 days respectively) against *E. coli*. The PP2 (0.10wt% FSP) showed remarkable antimicrobial activity against both strains. In contrast, PP3 (0.15wt% FSP) showed the highest activity (23 days) against *E. coli*. However, PP3 did not show any considerable activity against *B. subtilis* which could be attributed to the thickness of the cell wall of *B. subtilis*. *B. subtilis* exhibited a relatively denser outer membrane in contrast to *E. coli*. This possibly is the fact that *B. subtilis* showed greater resistance to the antimicrobial activity of hydrogels as compared to *E. coli* which exhibited a considerably greater sensitivity towards pectin-PVP/3-APDEMS sepiolite based hydrogels. The hydrogels generated pores in the cytoplasmic membrane of bacteria which caused the leakage of cytoplasmic material leading to cell death (Carson et al., 2002; Guerra-Rosas et al., 2017). The hydrogels possibly caused cell surface disintegration and irregular cellular boundaries. This restricted the growth of microbes around the hydrogel samples (**Figure 5**). The carboxylic group (-COOH) of pectin deprotonated when interacted with the bacterial cells. The -COOH was converted into carboxylate ion (COO^-) and H^+ ions. The H^+ ions caused the change in pH of the bacterial cells. This change in pH disrupted the bacterial cell wall while carboxylate ions inhibited cellular activities by binding with positive species of

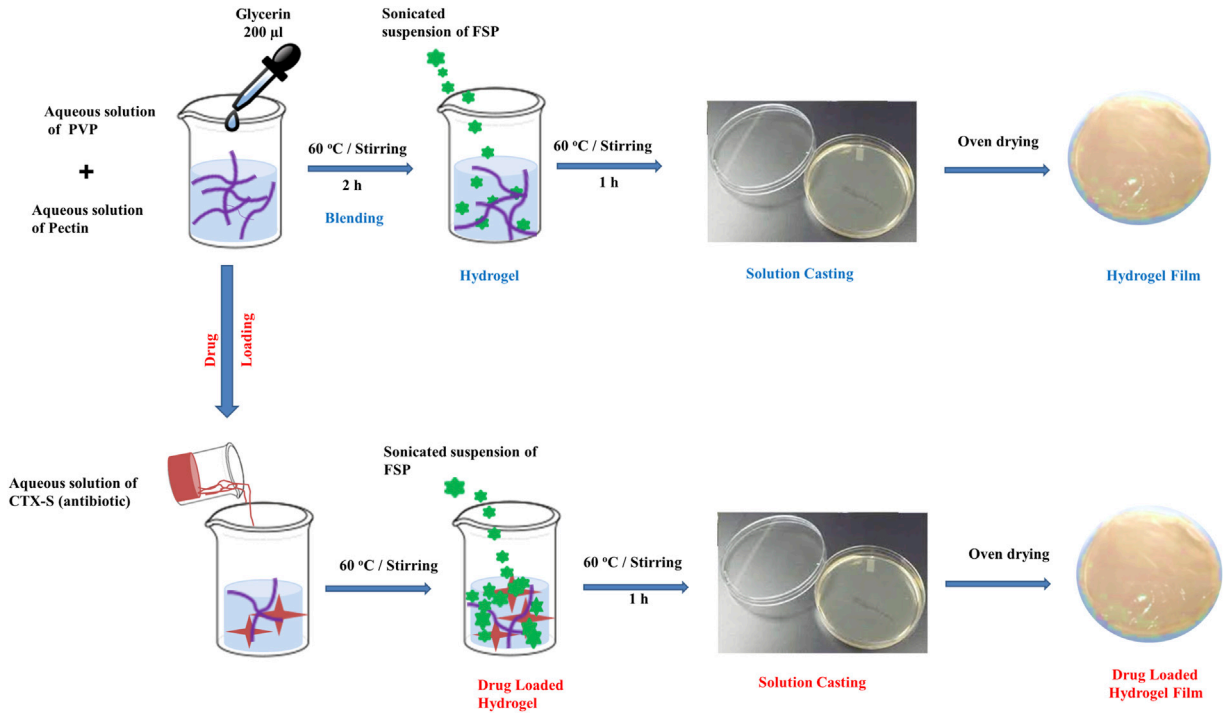

FIGURE 10 | Fabrication of hydrogel films

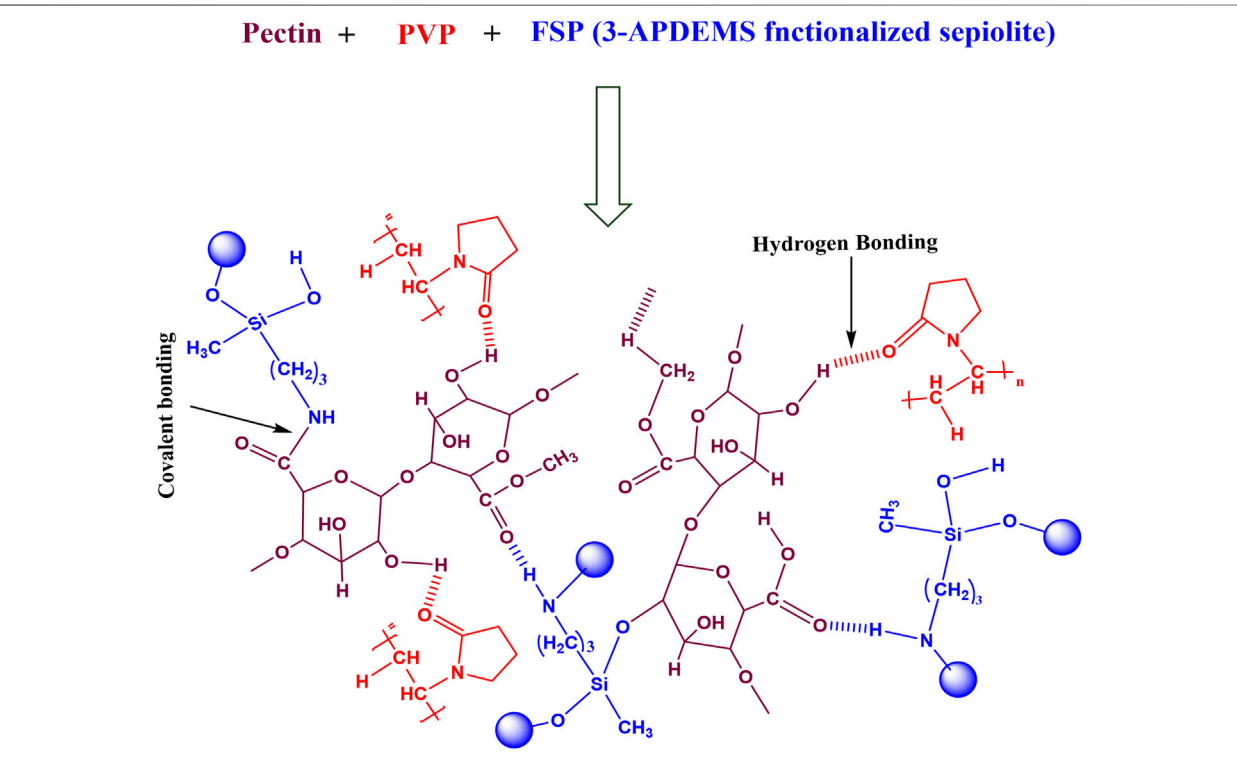

FIGURE 11 | Proposed crosslinked Pectin-PVP-FSP hydrogel matrix

bacterial cell (Kundukad et al., 2017). Overall, the films with large amount of modified clay possessed a higher antimicrobial potential. This property indicates that these hydrogels would enhance the anti-microbial potential of anti-biotics and could be used for wound healing applications.

3.6 Cytotoxicity Studies

To determine the impact of hydrogel on cell survival XTT assay was performed on 3T3 mouse fibroblast cell line. Hydrogel cytotoxicity was assessed by cell viability after 12, 48, and 72 hrs. ANOVA paired with Tukey's test was performed using SPSS software (version 17.0) for the validation of results. The results are presented in **Figure 6** which showed cell viability in PPC (75.87 ± 7.0%), PP1 (35.59 ± 3.44%), PP2 (45.64 ± 8.32%), and PP3 (57.67 ± 2.98%) groups as compared to control group (3T3 mouse fibroblast cells seeded without hydrogels) which is presented as doted bar (100 ± 0.0%) after 24 h. However, the viability of cells in different groups progressively increased with time (after 48 and 72 h). After 72 h, cell viability was significantly increased up to (111.08 ± 3.31%) in PPC (77.61 ± 4.46%) in PP1 (82.93 ± 4.59%) in PP2, and (80.85 ± 9.85%) in PP3. Furthermore, the results indicated that hydrogel supports the proliferation of cells even after 48 and 72 h as depicted by progressive increase in the percentage of viable cells in all groups (PPC, PP1, PP2, and PP3). The cell viability of all hydrogels was above 75% after 72 h (considered as non-cytotoxic) which indicated that PPC, PP1, PP2, and PP3 hydrogels are cytocompatible (Mishra et al., 2008).

Hydrogels have been used to efficiently deliver the seeded cells to the wound bed in a sustained and controlled manner (da Silva et al., 2019; Zhou et al., 2020). Hydrogel scaffolds allow sufficient transference of gases, nutrients, and growth factors to promote adhesion, retention, and survival of cells while reduce the microenvironmental shock and attack by host immune response in order to maximize the therapeutic capacity of cells (Garg et al., 2012; Nezhad-Mokhtari et al., 2019). Hydrogel is considered biodegradable, cytologically compatible, non-antigenic, ECM mimic, anti-microbial, and has the ability to maintain cellular potential (Xu et al., 2018).

The increase in cell proliferation after 72 h indicates that hydrogels understudy can play a crucial role in tissue engineering application as well.

3.7 Release Analysis of CTX-S

The pH-dependent release of drug was studied by immersing the CTX-S loaded hydrogel in PBS (pH 7.4), SIF (pH 6.8), and SGF (pH 1.2) to investigate the use of hydrogel for injectable drug delivery and controlled release application. PP2 was chosen as the host drug carrier over other hydrogels due to good swelling behavior in the buffer, good antimicrobial potential, and optimum biodegradability. The host drug carrier PP2 (0.10wt % FSP) was loaded with CTX-S and its release profile was examined in PBS (pH 7.4), SGF (pH 1.2), and SIF (pH 6.8) with time at 37°C according to the method described by Butt, et al. (2019) (Islam and Yasin, 2012; Butt et al., 2019). **Figure 7** demonstrated the drug release results showing a linear release of CTX-S in PBS. The drug release was remained steady as 91.82% drug was released in 2 h and 20 min. **Figure 7** demonstrates that release of drug was dependent on pH of buffer media, as the release of CTX-S was found consistent in PBS (pH 7.4) as compared to SIF (pH 6.8) and SGF (pH 1.2) which was in agreement with the pH-dependent swelling data (**section 3.3.2**). The results indicated that swelling has a dominating role in the release of drug via diffusion. In accordance with pH swelling results (**section 3.3.2**), the hydrogel showed higher swelling in SIF (pH 6.8) resulted in the creation of larger pore size and osmotic pressure inside of hydrogel matrix hence, facilitating faster diffusion rate of drug from hydrogel to medium (Bukhari et al., 2015; Mahdavinia et al., 2017; Sabzi et al., 2020). In SIF, more than 90% drug was released in first 30 min. The hydrogel showed lower swelling (**section 3.3.2**) at pH 7.4 (PBS) than that of swelling at pH 6.8. The decreased swelling at pH 7.4 resulted in the slower and consistent diffusion rate of drug from hydrogel to medium with respect to time. **Figure 7** indicated the sustained release of drug in PBS at pH 7.4 (blood pH).

Three different drug release mechanisms have been reported in literature i.e. swelling, erosion, and diffusion. The swelling, and diffusion work in conjugation when the polymer matrix was placed in a solution with a huge concentration difference (Benita, 2005). In this study, the drug release followed the process of diffusion in a controlled manner. In SGF, 28.4% drug was released in the first 10 min which was not in conformity with the US pharmacopeia standard as reported that the release of the drug in SGF must not be >10% in the first 30 min. In SIF 97.4%, the drug was released in 30 min. The CTX-S release in PBS and SIF was accordant with US pharmacopeia standard which confirmed the release in PBS and SIF must be >80%.

The results show that by controlling the type of polymer used for hydrogel preparation and its response to the change in pH, the release of drug can be controlled. The present hydrogel is suitable for injectable delivery and controlled release of drug.

3.8 Chemical Activity

To investigate the effect of hydrogel on the chemical integrity of loaded drug, the chemical activity of pure CTX-S (in PBS as well as water) and after release from hydrogel (in PBS) was observed using a double beam UV-vis spectrophotometer (Bashir et al., 2018). **Figure 8** shows recorded UV-vis scan spectra of pure ceftriaxone sodium antibiotic drug (CTX-S) before and after release from the hydrogel. The maximum absorbance for all three samples was observed at wavelength 270 nm which was characteristic (lambda maximum) of CTX-S. A similar pattern of all spectral lines indicated that the respective model drug did not show any chemical bonding with the hydrogel matrix and has retained its chemical configuration after being released from the host carrier. Thus, the fabricated hydrogel proved to be an effective carrier for antibiotics and hydrophilic drugs.

4 CONCLUSION

The macro-porous structure composed of different entities offers a novel multifunctional system with desired properties capable to develop suitable drug delivery carriers. The pectin-PVP-FSP based novel biodegradable semi-IPN drug carriers

with varying amounts of FSP (3-APDEMS functionalized sepiolite clay) was successfully developed by the solution casting method. FTIR study demonstrated the modification of clay with 3-APDEMS and SEM revealed rod-like morphology of hydrogels with size ranging 10–50 μm. With an increase in the amount of crosslinker, the degree of water swelling decreased. PP2 and PP3 showed the least swelling rate in water and electrolytes (NaCl and $CaCl_2$). The formulations PP2 and PP3 with an increased amount of crosslinker showed less degree of biodegradation. Both PP2 and PP3 showed remarkable antimicrobial activity against *E. coli* with hollow zone diameter 23 and 18 mm respectively. While for *B. subtilis* PP2 showed the best antimicrobial activity with a hollow zone diameter of 16 mm. This depicted that PP2 was effective against G+ and G-bacteria. All the hydrogels proved to be cytocompatible. In buffer solutions, all hydrogels less swelling at pH 2 which comparatively increased with increase in pH of medium. The *in vitro* drug release study of CTX-S loaded in phosphate buffer saline (pH 7.4) indicated 91.82% release in 2 h and 20 min in a controlled manner. Both pure CTX-S and released CTX-S drug showed maximum absorbance at 270 nm illustrating no chemical interaction between carrier and loaded drug. These hydrogels provide a better profile for pH-dependent injectable delivery and controlled release of ceftriaxone sodium. The fabricated hydrogels exhibited pH sensitivity for controlled drug release behavior, biodegradability, low-cost fabrication route, and antimicrobial potential. These characteristics make these hydrogels an ideal applicant for the slow release of drugs in a controlled manner, injectable drug delivery, and wound healing and wound dressing applications. With slight modification, these could be considered as promising materials for delivery of polar compounds, scaffolding, tissue engineering, and cancer therapeutics in the future.

DATA AVAILABILITY STATEMENT

The original contributions presented in the study are included in the article/supplementary material, further inquiries can be directed to the corresponding authors.

AUTHOR CONTRIBUTIONS

SR: Investigation; Experimental work, Methodology, Conceptualization; Data curation, Roles/Writing—original draft. NR: Project administration; Resources. SK: Supervision, validation, software. AG: Formal analysis. AI: Supervision; Validation; Investigation; Visualization; Writing—review andamp; editing; Software. RK: Formal analysis. AM: Cytotoxicity analysis. HB: Cytotoxicity analysis. DH: Supervision; Validation; Visualization, review. MR: Validation; Visualization, review, editing.

ACKNOWLEDGMENTS

The author is highly obliged to the School of Chemistry, Institute of Polymer and Textile Engineering, and Institute of Biochemistry and Biotechnology, University of the Punjab, Lahore for providing lab facilities.

REFERENCES

Abrougui, M. M., Lopez-Lopez, M. T., and Duran, J. D. G (2019). Mechanical Properties of Magnetic Gels Containing Rod-like Composite Particles. *Phil. Trans. R. Soc. A.* 377 (2143):20180218. doi:10.1098/rsta.2018.0218

Aguiar, P. H. N., Fernandes, N. M. G. S., Zani, C. L., and Mourão, M. M. (2017). A High-Throughput Colorimetric Assay for Detection of Schistosoma Mansoni Viability Based on the Tetrazolium Salt XTT. *Parasit Vectors* 10 (1), 300–310. doi:10.1186/s13071-017-2240-3

Ahrabi, S. F., Madsen, G., Dyrstad, K., Sande, S. A., and Graffner, C. (2000). Development of Pectin Matrix Tablets for Colonic Delivery of Model Drug Ropivacaine. *Eur. J. Pharm. Sci.* 10 (1), 43–52. doi:10.1016/s0928-0987(99)00087-1

Andrews, G. P., Laverty, T. P., and Jones, D. S. (2009). Mucoadhesive Polymeric Platforms for Controlled Drug Delivery. *Eur. J. Pharmaceutics Biopharmaceutics* 71 (3), 505–518. doi:10.1016/j.ejpb.2008.09.028

Ayushi, V. M., and Mansi, U. P. (2018). Development and Validation of UV Spectrophotometric Method for the Estimation of Ceftriaxone Sodium in Nanoparticles. *Res. Article - Der. Pharma. Chemica.* 10 (3)

Bali, G. K., Singla, S., Kashyap, Y., Dumka, V. K., and Kalia, A. (2018). Preparation, Physico-Chemical Characterization and Pharmacodynamics of Ceftriaxone Loaded BSA Nanoparticles. *J. Nanomed Nanotechnol* 9 (509), 2. doi:10.4172/2157-7439.1000509

Basha, M. A.-F. (2010). Magnetic and Optical Studies on Polyvinylpyrrolidone Thin Films Doped with Rare Earth Metal Salts. *Polym. J.* 42 (9), 728–734. doi:10.1038/pj.2010.60

Bashir, S., Teo, Y. Y., Ramesh, S., and Ramesh, K. (2018). Synthesis and Characterization of Karaya Gum-G- Poly (Acrylic Acid) Hydrogels and *in vitro* Release of Hydrophobic Quercetin. *Polymer* 147, 108–120. doi:10.1016/j.polymer.2018.05.071

Benita, S. (2005). *Microencapsulation: Methods and Industrial Applications*. Florida, USA: CRC Press.

Bryaskova, R., Pencheva, D., Nikolov, S., and Kantardjiev, T. (2011). Synthesis and Comparative Study on the Antimicrobial Activity of Hybrid Materials Based on Silver Nanoparticles (AgNps) Stabilized by Polyvinylpyrrolidone (PVP). *J. Chem. Biol.* 4 (4), 185–191. doi:10.1007/s12154-011-0063-9

Bukhari, S. M. H., Khan, S., Rehanullah, M., and Ranjha, N. M. (20152015). Synthesis and Characterization of Chemically Cross-Linked Acrylic Acid/Gelatin Hydrogels: Effect of pH and Composition on Swelling and Drug Release. *Int. J. Polym. Sci.* 2015, 1–15. doi:10.1155/2015/187961

Butt, A., Jabeen, S., Nisar, N., Islam, A., Gull, N., Iqbal, S. S., et al. (2019). Controlled Release of Cephradine by Biopolymers Based Target Specific Crosslinked Hydrogels. *Int. J. Biol. Macromolecules* 121, 104–112. doi:10.1016/j.ijbiomac.2018.10.018

Carson, C. F., Mee, B. J., and Riley, T. V. (2002). Mechanism of Action of Melaleuca Alternifolia (tea Tree) Oil on *Staphylococcus aureus* Determined by Time-Kill, Lysis, Leakage, and Salt Tolerance Assays and Electron Microscopy. *Antimicrob. Agents Chemother.* 46 (6), 1914–1920. doi:10.1128/aac.46.6.1914-1920.2002

da Silva, L. P., Reis, R. L., Correlo, V. M., and Marques, A. P. (2019). Hydrogel-based Strategies to advance Therapies for Chronic Skin Wounds. *Annu. Rev. Biomed. Eng.* 21, 145–169. doi:10.1146/annurev-bioeng-060418-052422

Darder, M., Matos, C. R. S., Aranda, P., Gouveia, R. F., and Ruiz-Hitzky, E. (2017). Bionanocomposite Foams Based on the Assembly of Starch and Alginate with Sepiolite Fibrous clay. *Carbohydr. Polym.* 157, 1933–1939. doi:10.1016/j.carbpol.2016.11.079

Dutta, J., and Devi, N. (2021). Preparation, Optimization, and Characterization of Chitosan-Sepiolite Nanocomposite Films for Wound Healing. *Int. J. Biol. Macromolecules* 186, 244–254. doi:10.1016/j.ijbiomac.2021.07.020

Eid, M., El-Arnaouty, M. B., Salah, M., Soliman, E.-S., and Hegazy, E.-S. A. (2012). Radiation Synthesis and Characterization of Poly(vinyl alcohol)/poly(N-Vinyl-2-Pyrrolidone) Based Hydrogels Containing Silver Nanoparticles. *J. Polym. Res.* 19 (3), 9835. doi:10.1007/s10965-012-9835-3

Fares, M. M., Assaf, S. M., and Abul-Haija, Y. M. (2010). Pectin Grafted poly(N-Vinylpyrrolidone): Optimization Andin Vitrocontrollable Theophylline Drug Release. *J. Appl. Polym. Sci.* 117 (4), 1945–1954. doi:10.1002/app.32172

Garg, T., Singh, O., Arora, S., and Murthy, R. (2012). Scaffold: a Novel Carrier for Cell and Drug Delivery. *Crit. Rev. Ther. Drug Carrier Syst.* 29 (1), 1–63. doi:10.1615/critrevtherdrugcarriersyst.v29.i1.10

Ghasemiyeh, P., and Mohammadi-Samani, S. (2021). Polymers Blending as Release Modulating Tool in Drug Delivery. *Front. Mater.* 8, 752813. doi:10.3389/fmats.2021.752813

Giri, T. K., Thakur, D., Alexander, A., Ajazuddin, H., Badwaik, H., Tripathy, M., et al. (2013). Biodegradable IPN Hydrogel Beads of Pectin and Grafted Alginate for Controlled Delivery of Diclofenac Sodium. *J. Mater. Sci. Mater. Med.* 24 (5), 1179–1190. doi:10.1007/s10856-013-4884-7

Guerra-Rosas, M. I., Morales-Castro, J., Cubero-Márquez, M. A., Salvia-Trujillo, L., and Martín-Belloso, O. (2017). Antimicrobial Activity of Nanoemulsions Containing Essential Oils and High Methoxyl Pectin during Long-Term Storage. *Food Control* 77, 131–138. doi:10.1016/j.foodcont.2017.02.008

Gülmen, S. S. T., Güvel, E. A., and Kızılcan, N. (2015). Preparation and Characterization of Chitosan/polypyrrole/sepiolite Nanocomposites. *Procedia-Social Behav. Sci.* 195, 1623–1632. doi:10.1016/j.sbspro.2015.06.219

Gulrez, S. K. H., Al-Assaf, S., and Phillips, G. O. (2011). Hydrogels: Methods of Preparation, Characterisation and Applications. *Prog. Mol. Environ. Bioengineering-from Anal. Model. Tech. Appl.* 2, 117–150. doi:10.5772/24553

Hun Kim, M., Choi, G., Elzatahry, A., Vinu, A., Bin Choy, Y., and Choy, J.-H. (2016). Review of clay-drug Hybrid Materials for Biomedical Applications: Administration Routes. *Clays Clay Miner.* 64 (2), 115–130. doi:10.1346/ccmn.2016.0640204

Hussien, N. A., Işıklan, N., and Türk, M. 2018. Pectin-conjugated Magnetic Graphene Oxide Nanohybrid as a Novel Drug Carrier for Paclitaxel Delivery. *Artif. Cell Nanomedicine, Biotechnol.* 46 (Suppl. 1): 264–273. doi:10.1080/21691401.2017.1421211

Iglesias, N., Galbis, E., Valencia, C., Díaz-Blanco, M. J., Lacroix, B., and de-Paz, M.-V. (2020). Biodegradable Double Cross-Linked Chitosan Hydrogels for Drug Delivery: Impact of Chemistry on Rheological and Pharmacological Performance. *Int. J. Biol. Macromolecules* 165, 2205–2218. doi:10.1016/j.ijbiomac.2020.10.006

Islam, A., and Yasin, T. (2012). Controlled Delivery of Drug from pH Sensitive Chitosan/poly (Vinyl Alcohol) Blend. *Carbohydr. Polym.* 88 (3), 1055–1060. doi:10.1016/j.carbpol.2012.01.070

Jacob, B., Kloss, N., Böhle, S., Kirschberg, J., Zippelius, T., Heinecke, M., et al. (2020). Tranexamic Acid Is Toxic on Human Chondrocytes, *in vitro*. *J. Orthopaedics* 20, 1–5. doi:10.1016/j.jor.2019.12.008

Khramov, A. N., Balbyshev, V. N., Voevodin, N. N., and Donley, M. S. (2003). Nanostructured Sol–Gel Derived Conversion Coatings Based on Epoxy-And Amino-Silanes. *Prog. Org. Coat.* 47 (3-4), 207–213. doi:10.1016/s0300-9440(03)00140-1

Ko, W-K., Lee, S. J., Kim, S. J., Han, G. H., Han, I-b., Hong, J. B., et al. (2021). Direct Injection of Hydrogels Embedding Gold Nanoparticles for Local Therapy after Spinal Cord Injury. *Biomacromolecules* 22(7), 2887–2901. doi:10.1021/acs.biomac.1c00281

Kumar, M., Mishra, R. K., and Banthia, A. K. (2010). Development of Pectin Based Hydrogel Membranes for Biomedical Applications. *Int. J. Plast. Technol.* 14 (2), 213. doi:10.1007/s12588-011-0019-5

Kumar, R., Rahman, H., Ranwa, S., Kumar, A., and Kumar, G. (2020). Development of Cost Effective Metal Oxide Semiconductor Based Gas Sensor over Flexible Chitosan/PVP Blended Polymeric Substrate. *Carbohydr. Polym.* 239, 116213. doi:10.1016/j.carbpol.2020.116213

Kundukad, B., Schussman, M., Yang, K., Seviour, T., Yang, L., Rice, S. A., et al. (2017). Mechanistic Action of Weak Acid Drugs on Biofilms. *Sci. Rep.* 7 (1), 4783–4812. doi:10.1038/s41598-017-05178-3

Li, D-q., Li, J., Dong, H-l., Li, X., Zhang, J-q., Ramaswamy, S., et al. (2021). Pectin in Biomedical and Drug Delivery Applications: A Review. *Int. J. Biol. Macromolecules* 185, 49–65. doi:10.1016/j.ijbiomac.2021.06.088

Li, D.-q., Wang, S.-y., Meng, Y.-j., Li, J.-f., and Li, J. (2020). An Injectable, Self-Healing Hydrogel System from Oxidized Pectin/chitosan/γ-Fe2O3. *Int. J. Biol. Macromolecules* 164, 4566–4574. doi:10.1016/j.ijbiomac.2020.09.072

Liu, L., Fishman, M. L., Kost, J., and Hicks, K. B. (2003). Pectin-based Systems for colon-specific Drug Delivery via Oral Route. *Biomaterials* 24 (19), 3333–3343. doi:10.1016/s0142-9612(03)00213-8

Liu, P., Du, M., Clode, P., Li, H., Liu, J., and Leong, Y.-K. (2020). Surface Chemisty, Microstructure, and Rheology of Thixotropic 1-D Sepiolite Gels. *Clays Clay Miner.* 68 (1), 9–22. doi:10.1007/s42860-019-00050-z

Liu, S., Qamar, S. A., Qamar, M., Basharat, K., and Bilal, M. (2021). Engineered Nanocellulose-Based Hydrogels for Smart Drug Delivery Applications. *Int. J. Biol. Macromolecules* 181, 275–290. doi:10.1016/j.ijbiomac.2021.03.147

Mahdavinia, G. R., Mosallanezhad, A., Soleymani, M., and Sabzi, M. (2017). Magnetic- and pH-Responsive κ-carrageenan/chitosan Complexes for Controlled Release of Methotrexate Anticancer Drug. *Int. J. Biol. Macromolecules* 97, 209–217. doi:10.1016/j.ijbiomac.2017.01.012

Marandi, G. B., Esfandiari, K., Biranvand, F., Babapour, M., Sadeh, S., and Mahdavinia, G. R. (2008). pH Sensitivity and Swelling Behavior of Partially Hydrolyzed Formaldehyde-Crosslinked Poly(acrylamide) Superabsorbent Hydrogels. *J. Appl. Polym. Sci.* 109 (2), 1083–1092. doi:10.1002/app.28205

Mathew, S. (2018). Comparative Evaluation of Antimicrobial Efficacy of Neem and Ginger, to Prove its Effectiveness in Decontaminating "Gutta Percha Cones"-An *in vitro* Study. *Int. J. Contemp. Res. Rev.* 9 (01). doi:10.15520/ijcrr/2018/9/01/400

Mirzaei B., E., Ramazani S. A., A., Shafiee, M., and Danaei, M. (2013). Studies on Glutaraldehyde Crosslinked Chitosan Hydrogel Properties for Drug Delivery Systems. *Int. J. Polymeric Mater. Polymeric Biomater.* 62 (11), 605–611. doi:10.1080/00914037.2013.769165

Mishra, R. K., Datt, M., and Banthia, A. K. (2008). Synthesis and Characterization of Pectin/PVP Hydrogel Membranes for Drug Delivery System. *Aaps Pharmscitech* 9 (2), 395–403. doi:10.1208/s12249-008-9048-6

Muller, M. J., Hollyoak, M. A., Moaveni, Z., Brown, T. L. H., Herndon, D. N., and Heggers, J. P. (2003). Retardation of Wound Healing by Silver Sulfadiazine Is Reversed by Aloe Vera and Nystatin. *Burns* 29 (8), 834–836. doi:10.1016/s0305-4179(03)00198-0

Naeem, F., Khan, S., Jalil, A., Ranjha, N. M., Riaz, A., Haider, M. S., et al. (2017). pH Responsive Cross-Linked Polymeric Matrices Based on Natural Polymers: Effect of Process Variables on Swelling Characterization and Drug Delivery Properties. *Bioimpacts* 7 (3), 177–192. doi:10.15171/bi.2017.21

Nandiyanto, A. B. D., Oktiani, R., and Ragadhita, R. (2019). How to Read and Interpret FTIR Spectroscope of Organic Material. *Indonesian J. Sci. Technol.* 4 (1), 97–118. doi:10.17509/ijost.v4i1.15806

Nešić, A., Onjia, A., Davidović, S., Dimitrijević, S., Errico, M. E., Santagata, G., et al. (2017). Design of Pectin-Sodium Alginate Based Films for Potential Healthcare Application: Study of Chemico-Physical Interactions between the Components of Films and Assessment of Their Antimicrobial Activity. *Carbohydr. Polym.* 157, 981–990. doi:10.1016/j.carbpol.2016.10.054

Nezhad-Mokhtari, P., Ghorbani, M., Roshangar, L., and Soleimani Rad, J. (2019). A Review on the Construction of Hydrogel Scaffolds by Various Chemically Techniques for Tissue Engineering. *Eur. Polym. J.* 117, 64–76. doi:10.1016/j.eurpolymj.2019.05.004

Nieto-Suárez, M., Palmisano, G., Ferrer, M. L., Gutiérrez, M. C., Yurdakal, S., Augugliaro, V., et al. (2009). Self-assembled Titania–Silica–Sepiolite Based Nanocomposites for Water Decontamination. *J. Mater. Chem.* 19 (14), 2070–2075. doi:10.1039/B813864H

Palem, R. R., Rao, K. M., Shimoga, G., Saratale, R. G., Shinde, S. K., Ghodake, G. S., et al. (2021). Physicochemical Characterization, Drug Release, and Biocompatibility Evaluation of Carboxymethyl Cellulose-Based Hydrogels Reinforced with Sepiolite Nanoclay. *Int. J. Biol. Macromolecules* 178, 464–476. doi:10.1016/j.ijbiomac.2021.02.195

Peers, S., Montembault, A., and Ladavière, C. (2020). Chitosan Hydrogels for Sustained Drug Delivery. *J. Controlled Release* 326, 150–163. doi:10.1016/j.jconrel.2020.06.012

Pierce, A., Zheng, Y., Wagner, W. L., Scheller, H. V., Mohnen, D., Ackermann, M., et al. (2020). Visualizing Pectin Polymer-Polymer Entanglement Produced by Interfacial Water Movement. *Carbohydr. Polym.* 246, 116618. doi:10.1016/j.carbpol.2020.116618

Rahman, M. R., Chang Hui, J. L., and Hamdan, S. b. (2018). "Introduction and Reinforcing Potential of Silica and Various clay Dispersed Nanocomposites," in *Silica and Clay Dispersed Polymer Nanocomposites* (Amsterdam, Netherlands: Elsevier), 1–24. doi:10.1016/b978-0-08-102129-3.00001-4

Rasool, A., Ata, S., and Islam, A. (2019). Stimuli Responsive Biopolymer (Chitosan) Based Blend Hydrogels for Wound Healing Application. *Carbohydr. Polym.* 203, 423–429. doi:10.1016/j.carbpol.2018.09.083

Rasool, N., Yasin, T., Heng, J. Y. Y., and Akhter, Z. (2010). Synthesis and Characterization of Novel pH-, Ionic Strength and Temperature- Sensitive Hydrogel for Insulin Delivery. *Polymer* 51 (8), 1687–1693. doi:10.1016/j.polymer.2010.02.013

Raza, M. A., Jeong, J.-O., and Park, S. H. (2021). State-of-the-Art Irradiation Technology for Polymeric Hydrogel Fabrication and Application in Drug Release System. *Front. Mater.* 8, 769436. doi:10.3389/fmats10.3389/fmats.2021.769436

Rinoldi, C., Lanzi, M., Fiorelli, R., Nakielski, P., Zembrzycki, K., Kowalewski, T., et al. (2021). Three-Dimensional Printable Conductive Semi-Interpenetrating Polymer Network Hydrogel for Neural Tissue Applications. *Biomacromolecules* 22(7), 3084–3098. doi:10.1021/acs.biomac.1c00524

Roy, N., Saha, N., Kitano, T., and Saha, P. (2010). Novel Hydrogels of PVP–CMC and Their Swelling Effect on Viscoelastic Properties. *J. Appl. Polym. Sci.* 117 (3), 1703–1710. doi:10.1002/app.32056

Ruiz-Hitzky, E., Aranda, P., Darder, M., and Rytwo, G. (2010). Hybrid Materials Based on Clays for Environmental and Biomedical Applications. *J. Mater. Chem.* 20 (42), 9306–9321. doi:10.1039/c0jm00432d

Sabzi, M., Afshari, M. J., Babaahmadi, M., and Shafagh, N. (2020). pH-Dependent Swelling and Antibiotic Release from Citric Acid Crosslinked Poly(vinyl Alcohol) (PVA)/nano Silver Hydrogels. *Colloids Surf. B: Biointerfaces* 188, 110757. doi:10.1016/j.colsurfb.2019.110757

Saeedi Garakani, S., Davachi, S. M., Bagher, Z., Heraji Esfahani, A., Jenabi, N., Atoufi, Z., et al. (2020). Fabrication of Chitosan/polyvinylpyrrolidone Hydrogel Scaffolds Containing PLGA Microparticles Loaded with Dexamethasone for Biomedical Applications. *Int. J. Biol. Macromolecules* 164, 356–370. doi:10.1016/j.ijbiomac.2020.07.138

Sanaeepur, H., Mashhadikhan, S., Mardassi, G., Ebadi Amooghin, A., Van der Bruggen, B., and Moghadassi, A. (2019). Aminosilane Cross-Linked Poly Ether-Block-Amide PEBAX 2533: Characterization and CO2 Separation Properties. *Korean J. Chem. Eng.* 36 (8), 1339–1349. doi:10.1007/s11814-019-0323-x

Shafiq, M., Yasin, T., and Saeed, S. (2012). Synthesis and Characterization of Linear Low-Density Polyethylene/sepiolite Nanocomposites. *J. Appl. Polym. Sci.* 123 (3), 1718–1723. doi:10.1002/app.34633

Sharma, R., and Ahuja, M. (2011). Thiolated Pectin: Synthesis, Characterization and Evaluation as a Mucoadhesive Polymer. *Carbohydr. Polym.* 85 (3), 658–663. doi:10.1016/j.carbpol.2011.03.034

Shirazi, N. M., Eslahi, N., and Gholipour-Kanani, A. (2021). Production and Characterization of Keratin/Tragacanth Gum Nanohydrogels for Drug Delivery in Medical Textiles. *Front. Mater* 8, 371. doi:10.3389/fmats.2021.720385

Singh, B., and Singh, B. (2020). Graft Copolymerization of Polyvinylpyrollidone onto Azadirachta indica Gum Polysaccharide in the Presence of Crosslinker to Develop Hydrogels for Drug Delivery Applications. *Int. J. Biol. Macromolecules* 159, 264–275. doi:10.1016/j.ijbiomac.2020.05.091

Sivagangi Reddy, N., Madhusudana Rao, K., Sudha Vani, T. J., Krishna Rao, K. S. V., and Lee, Y. I. (2016). Pectin/poly(acrylamide-co-acrylamidoglycolic Acid) pH Sensitive Semi-IPN Hydrogels: Selective Removal of Cu2+and Ni2+, Modeling, and Kinetic Studies. *Desalination Water Treat.* 57 (14), 6503–6514. doi:10.1080/19443994.2015.1008053

Sizílio, R. H., Galvão, J. G., Trindade, G. G. G., Pina, L. T. S., Andrade, L. N., Gonsalves, J. K. M. C., et al. (2018). Chitosan/pvp-based Mucoadhesive Membranes as a Promising Delivery System of Betamethasone-17-Valerate for Aphthous Stomatitis. *Carbohydr. Polym.* 190, 339–345.

Sohail, K., Khan, I. U., Shahzad, Y., Hussain, T., and Ranjha, N. M. (2014). pH-Sensitive Polyvinylpyrrolidone-Acrylic Acid Hydrogels: Impact of Material Parameters on Swelling and Drug Release. *Braz. J. Pharm. Sci.* 50 (1), 173–184. doi:10.1590/s1984-82502011000100018

Song, F., Gong, J., Tao, Y., Cheng, Y., Lu, J., and Wang, H. (2021). A Robust Regenerated Cellulose-Based Dual Stimuli-Responsive Hydrogel as an Intelligent Switch for Controlled Drug Delivery. *Int. J. Biol. Macromolecules* 176, 448–458. doi:10.1016/j.ijbiomac.2021.02.104

Song, Y.-J., Wang, M., Zhang, X.-Y., Wu, J.-Y., and Zhang, T. (2014). Investigation on the Role of the Molecular Weight of Polyvinyl Pyrrolidone in the Shape Control of High-Yield Silver Nanospheres and Nanowires. *Nanoscale Res. Lett.* 9 (1), 17. doi:10.1186/1556-276x-9-17

Sriamornsak, P., Thirawong, N., Nunthanid, J., Puttipipatkhachorn, S., Thongborisute, J., and Takeuchi, H. (2008). Atomic Force Microscopy Imaging of Novel Self-Assembling Pectin-Liposome Nanocomplexes. *Carbohydr. Polym.* 71 (2), 324–329. doi:10.1016/j.carbpol.2007.05.027

Tanc, B., and Orakdogen, N. (2019). Insight into (Alkyl)methacrylate-based Copolymer/sepiolite Nanocomposite Cryogels Containing Amino and Sulfonic Acid Groups: Optimization of Network Properties and Elasticity via Cryogelation Process. *Reactive Funct. Polym.* 140, 31–47. doi:10.1016/j.reactfunctpolym.2019.03.022

Veronovski, A., Tkalec, G., Knez, Ž., and Novak, Z. (2014). Characterisation of Biodegradable Pectin Aerogels and Their Potential Use as Drug Carriers. *Carbohydr. Polym.* 113, 272–278. doi:10.1016/j.carbpol.2014.06.054

Xu, Y., Li, Y., Chen, Q., Chen, Q., Fu, L., Tao, L., et al. (2018). Injectable and Self-Healing Chitosan Hydrogel Based on Imine Bonds: Design and Therapeutic Applications. *Int. J. Mol. Sci.* 19 (8), 2198. doi:10.3390/ijms19082198

Xu, Z., Liu, Q., and Finch, J. A. (1997). Silanation and Stability of 3-aminopropyl Triethoxy Silane on Nanosized Superparamagnetic Particles: I. Direct Silanation. *Appl. Surf. Sci.* 120 (3-4), 269–278. doi:10.1016/s0169-4332(97)00234-1

Yang, X., Chen, L., Huang, B., Bai, F., and Yang, X. (2009). Synthesis of pH-Sensitive Hollow Polymer Microspheres and Their Application as Drug Carriers. *Polymer* 50 (15), 3556–3563. doi:10.1016/j.polymer.2009.06.027

Yasin, T., Rasool, N., and Akhter, Z. (2008). Synthesis of Carboxymethyl-Chitosan/acrylic Acid Hydrogel Using Silane Crosslinker. *e-Polymers* 8 (1). doi:10.1515/epoly.2008.8.1.1636

Zhou, S., Wang, Y., Zhang, K., Cao, N., Yang, R., Huang, J., et al. (2020). The Fabrication and Evaluation of a Potential Biomaterial Produced with Stem Cell Sheet Technology for Future Regenerative Medicine. *Stem Cells Int* 2020, 9567362. doi:10.1155/2020/9567362

Zu, G., Kanamori, K., Nakanishi, K., Lu, X., Yu, K., Huang, J., et al. (2019). Superelastic Multifunctional Aminosilane-Crosslinked Graphene Aerogels for High thermal Insulation, Three-Component Separation, and Strain/pressure-Sensing Arrays. *ACS Appl. Mater. Inter.* 11 (46), 43533–43542. doi:10.1021/acsami.9b16746

Conflict of Interest: The authors declare that the research was conducted in the absence of any commercial or financial relationships that could be construed as a potential conflict of interest.

Publisher's Note: All claims expressed in this article are solely those of the authors and do not necessarily represent those of their affiliated organizations, or those of the publisher, the editors and the reviewers. Any product that may be evaluated in this article, or claim that may be made by its manufacturer, is not guaranteed or endorsed by the publisher.